Postprint of Plant Science Volume 252, November 2016, Pages 42–52
http://dx.doi.org/10.1016/j.plantsci.2016.07.002

Sunflower *Ha*GPAT9-1 is the predominant GPAT during seed development

Miriam Payá-Milans[1,2]; Jose Antonio Aznar-Moreno[1,3]; Tiago S. Balbuena[4,5]; Richard P. Haslam[6]; Satinder K. Gidda[7]; Javier Pérez-Hormaeche[1]; Robert T. Mullen[7]; Jay J. Thelen[4]; Johnathan A. Napier[6]; Joaquín J. Salas[1]; Rafael Garcés[1]; Enrique Martínez-Force[1]; Mónica Venegas-Calerón[1]†

[1] Instituto de la Grasa (CSIC), Campus Universitario Pablo de Olavide, 41013 Sevilla, Spain.

[2] Department of Entomology & Plant Pathology, University of Tennessee, Knoxville, Tennessee 37996.

[3] Department of Biochemistry & Molecular Biophysics, Kansas State University, Manhattan, Kansas 66506.

[4] Department of Biochemistry and Interdisciplinary Plant Group, University of Missouri, Columbia, Missouri 65211.

[5] Department of Technology, São Paulo State University, Jaboticabal, São Paulo, Brazil.

[6] Department of Biological Chemistry and Crop Protection, Rothamsted Research, Harpenden, Hertfordshire AL5 2JQ, United Kingdom.

[7] Department of Molecular and Cellular Biology, University of Guelph, Guelph, Ontario, N1G 2W1 Canada.

† To whom correspondence should be addressed.

Corresponding author:

Mónica Venegas-Calerón, Instituto de la Grasa (CSIC), Campus Universitario Pablo de Olavide, 41013 Sevilla, Spain. Email: mvc@ig.csic.es; Tlf: +34 954611550-259.

Date of submission: April 22, 2016

Number of tables and figures: 3 tables and 7 figures (in color online-only)

Supplementary Data: 3 tables, 3 figures, 1 methods

HIGHLIGHT:

A GPAT9 homologue identified in the sunflower seed proteome is active *in vivo* and *in vitro*, and it can modify the lipid content of yeast. The activity of a second isoform remains unclear.

Abstract

In oil crops, triacylglycerol biosynthesis is an important metabolic pathway in which glycerol-3-phosphate acyltransferase (GPAT) performs the first acylation step. Mass spectrometry analysis of developing sunflower (*Helianthus annuus*) seed membrane fractions identified an abundant GPAT, *Ha*GPAT9 isoform 1, with a N-terminal peptide that possessed two phosphorylated residues with possible regulatory function. *Ha*GPAT9-1 belongs to a broad eukaryotic GPAT family, similar to mammalian GPAT3, and it represents one of the two sunflower GPAT9 isoforms, sharing 90% identity with *Ha*GPAT9-2. Both sunflower genes are expressed during seed development and in vegetative tissues, with *HaGPAT9-1* transcripts accumulating at relatively higher levels than those for *HaGPAT9-2*. Green fluorescent protein tagging of *Ha*GPAT9-1 confirmed its subcellular accumulation in the endoplasmic reticulum. Despite their overall sequence similarities, the two sunflower isoforms displayed some differences in their enzymatic activities. For instance, *Ha*GPAT9-1 possesses *in vivo* GPAT activity that rescues the lethal phenotype of the cmy228 yeast strain, while *in vitro* assays revealed a preference of *Ha*GPAT9-1 for palmitoyl-, oleoyl- and linoleoyl-CoAs of one order of magnitude, with the highest increase in yield for oleoyl- and linoleoyl-CoAs. By contrast, no enzymatic activity could be detected for *Ha*GPAT9-2, even though its over-expression modified the TAG profile of yeast.

Keywords: Endoplasmic reticulum; Glycerol-3-phosphate acyltransferase; *Helianthus annuus*; Mass spectrometry; Triacylglycerol; Yeast.

Abbreviations:

ACP, acyl carrier protein

ConA, Concanavalin A

DAF, days after flowering

ER, endoplasmic reticulum

FOA, fluoroorotic acid

G3P, glycerol-3-phosphate

GFP, green fluorescent protein

GPAT, glycerol-3-phosphate acyltransferase

LPA, 1-acylglycerol-3-phosphate or lysophosphatidic acid

LPAAT, 1-acylglycerol-3-phosphate acyltransferase

PDAT, phosphatidylcholine:diacylglycerol acyltransferase

TAG, triacylglycerol

1. Introduction

Glycerol-3-phosphate acyltransferases (GPAT; E.C. 2.3.1.15) are enzymes that transfer the acyl moiety from an acyl-coenzyme A (CoA) donor (or acyl-acyl carrier protein [ACP] in plastids) to the *sn*-1 position of a glycerol-3-phosphate (G3P) molecule, yielding 1-acylglycerol-3-phosphate (or lysophosphatidic acid, LPA) [1]. This first acylation step occurs slower than the second [2], limiting the availability of LPA and producing a potential 'bottleneck' in the flow of carbon into glycerolipids, as originally defined by Eugene Kennedy [3].

It is now realized that GPAT-mediated regulation of glycerolipid synthesis is more complex than previously thought. Considerable effort has been dedicated to determine the major plant GPAT isoforms implicated in seed oil synthesis, leading to the identification of GPAT sequences from three protein families in different plant species [4,5,6]. The GPAT family homologue of GPAT9 (At5g60620) from *Arabidopsis thaliana* L. has been attributed a direct role in TAG biosynthesis [7,8]. This enzyme is located in the endoplasmic reticulum (ER) and its protein sequence shares certain similarity with mammalian GPAT3 and GPAT4, both of which are involved in lipid storage in white adipose tissue of the liver and mammary glands [9].

There have been several attempts to purify plant GPATs from ER fractions. For instance, partial purification of a solubilized GPAT from

avocado mesocarp (*Persea americana* Mill.) was achieved by affinity chromatography Eccleston and Harwood [10], although the purified enzyme was very unstable. A GPAT from palm callus (*Elaeis guineensis* Jacq.) was also partially purified using ion exchange and molecular exclusion chromatography Manaf and Harwood [11]. Based on this latter approach, Ruiz-Lopez *et al*. [12] fractions from sunflower (*Helianthus annuus* L.) enriched in microsomal GPAT activity were obtained, although the enzyme responsible for that activity was not successfully sequenced.

Common sunflower seeds accumulate high levels of TAGs that are rich in oleic and linoleic acids [13]. Moreover, several mutant sunflower lines have been selected and bred to produce oils with diverse properties and fatty acid content [13]. The study of the genetics and biochemistry of oil biosynthesis in sunflower seeds not only provides a basic understanding of the underlying processes but also, it yields potential targets to customize the lipid composition of sunflower oil in order to improve both oil quality and production. As such, the GPAT activity in developing seed embryos was characterized, whereby the highest activity was measured in seeds between 15-20 days after flowering (DAF), showing specificity towards palmitoyl-CoA, oleoyl-CoA and linoleoyl-CoA derivatives [12]. The results of this study reflected the fatty acid composition at the *sn*-1 position of sunflower TAGs, supporting the involvement of this activity in oil assembly. To complement this earlier

study, we report here the successful identification of the major GPAT isoform present in developing sunflower seed membranes, as well as its molecular and biochemical characterization. The role of this enzyme in sunflower oil synthesis is discussed in view of these findings.

2. Materials and Methods

2.1. Biological material and growth conditions

The wild-type CAS-6 sunflower (*H. annuus*) line (Sunflower Collection of Instituto de la Grasa, CSIC, Spain) was grown as described in Ruiz-Lopez *et al*. [12]. Root, hypocotyl, leaf tissues and seeds at different days after flowering (DAF) from at least three plants were harvested for downstream analyses. *S. cerevisiae* strains were grown at 22°C in restricted SC medium supplemented with glucose, galactose or raffinose (2%, w/v). Tobacco (*Nicotiana tabacum* L.) Bright Yellow-2 (BY-2) cells were cultured in suspension and prepared as described elsewhere [7]. The strains and plasmids used in this study are described in Table 1.

For heterologous expression studies and complementation assays, the PLATE transformation method [21] was used to separately introduce the plasmid constructs into the yeast strains. Yeast transformants were grown at 30ºC overnight in liquid selective SC medium (SC-U for pYES2 and SC-L for p416) supplemented with 2% galactose. Complementation assays were performed on 5 μL aliquots of serial dilutions plated on various selective media and incubated at 22 ºC. Yeast transformed with the empty plasmids were used as controls.

2.2. Cloning and expression of HaGPAT9s

Sunflower *HaGPAT9* isoforms 1 and 2 were identified based on a BLAST search of *Helianthus* sp. EST sequences using human GPAT3 as the query. Alignments from these ESTs revealed two complete GPAT sequences in sunflower, which were amplified from 15 DAF sunflower seed cDNA using specific primer pairs (HaGPAT9_[1,2]-F/-R: Electronic Material Table S1). The sequences of these cDNAs were confirmed (Secugen, Madrid, Spain) and complete sequences for *HaGPAT9-1* and *2* were deposited in GenBank under accession numbers EF552845 and EF552846, respectively.

Full-length sequences were amplified using the GPAT9_[1,2]pYES2-F/-R primer pairs (Table S1) and they were cloned into the pYES2(*URA3*) galactose inducible vector (Invitrogen, Carlsbad, CA, USA). Alternatively, the GPAT9_[1,2]p416-F/-R primer pairs were used for constitutive expression in the yeast p416(*LEU2*) vector [19] (kindly provided by Dr Ana Rincón). Quantitative PCR was performed using cDNA from seeds and tissues obtained at various DAF, as described in Sánchez-García *et al*. [22], and using the qGPAT9_[1,2]-F/-R primers (Table S1) and the corresponding constructs in the pYES2 plasmid.

2.3. Mass spectrometry analysis of sunflower seed proteins

Solubilized proteins from sunflower seed microsomal fractions were analyzed on the LTQ-Orbitrap XL mass spectrometer (Methods S1). The resulting spectra were searched against a custom sunflower database containing data from NCBI, TIGR and UniGene, as well as from the sunflower acyltransferases cloned to date that were added manually.

2.4. Confocal microscopy of GFP-tagged HaGPAT9-1 in tobacco cell suspensions

The full-length open reading frame (ORF, minus the stop codon) of *Ha*GPAT9-1 was amplified by PCR using GPAT9_1pUC18-F/-R primers, designed with *Nhe*I restriction sites (Table S1). Cloned products were inserted into the unique *Nhe*I restriction site of pUC18/*Nhe*I-mGFP [20]. The resulting construct encoded *Ha*GPAT9-1 linked at its C terminus to the monomeric green fluorescent protein (GFP).

Tobacco cells were transiently transformed with the plasmid encoding *Ha*GPAT9-1-GFP as described previously [7]. The cells were then fixed and stained during the final 20 min of incubation with Alexa Fluor 594 conjugated Concanavalin A (ConA) [23] at a final concentration of 5 mg/mL (Molecular probes, Eugene, OR, USA). Confocal laser scanning microscopy (CLSM) images of the BY-2 cells were acquired on a Leica DM RBE microscope using a 63x Plan Apochromat oil-immersion objective, a TCS SP2 scanning head (Leica Microsystems, Germany) and

the LEICA TCN NT software package (Version 2.61). GFP was excited at 488 nm with an argon laser and with an emission filter opening at 480-550 nm. Images of the cells were deconvoluted, and adjusted for brightness and contrast using Northern Eclipse 5.0 software (Empix Imaging, Canada). The images are representative of >20 cells from at least three independent transformation experiments and they were generated using Adobe Photoshop CS (Adobe Systems, San Jose, CA, USA).

2.5. Computational analysis

Phosphorylation sites were predicted using the GPS 3.0 server [24]. Protein sequences were aligned using Clustal Omega (version 1.2.1) from the EMBL-EBI server [25, 26], applying the default settings. Gene ontology (GO) assignments were made using Blast2GO 3.2 [27] from their closest GO-annotated orthologs in the plant NR database using default settings. A phylogenetic tree was constructed from the alignment using the minimum evolution method in the MEGA 5.0 program and with a bootstrap value of 1000 [28]. The programs used to predict the subcellular localization of sunflower *Ha*GPAT9-1 were TargetP1.1 (www.cbs.dtu.dk/services/TargetP/) and ChloroP1.1 (www.cbs.dtu.dk/services/ChloroP/). The program used to identify target regions that could potentially be disrupted by translational fusion to the GFP was TMHMM (www.cbs.dtu.dk/services/TMHMM-2.0/). The OCTOPUS program (http://octopus.cbr.su.se/) was used to identify putative

transmembrane regions. Statistical significance between control replicates and samples was obtained using Student's t-test with $P<0.05$.

2.6. Analysis of the TAG and fatty acid composition of yeast cells

gat1Δ yeast strain transformed with a pYES2 construct either containing a GPAT or empty was grown in SC-U selective media (see Methods S1 for details). Overnight cultures were used to inoculate galactose-containing media to induce enzyme expression. After 24h growth, cells were harvested, washed and dried under nitrogen current. The cell pellet was resuspended in methanol and heated at 80ºC for 10 min. Then, total lipids were extracted (Methods S1) and subjected to TAG purification [29]. The molecular TAG species were analyzed by MS as described in Hamilton *et al*. [30]. The data were normalized to dry cell weight using the internal standard tri15:0 (Nu-Check Prep, Elysian, MN, USA).

2.7. Preparation of yeast microsomal fractions

Yeast cells transformed with different pYES2 constructs were harvested from 50 mL cultures of yeasts, and they were resuspended in 0.5 mL of a lysis solution containing 50 mM HEPES [pH 7.0], 2 mM EDTA and 10% (v/v) glycerol. An equivalent volume of 0.4-0.6 mm acid treated glass beads (Sigma-Aldrich, St. Louis, MO, USA) were added to the cells and they were subjected to six cycles of 30 s grinding in a MiniBeadbeater-8

(BioSpec, Bartlesville, OK, USA) and left for 1 min on ice. The homogenate was spun at 600 g for 5 min and the supernatant was collected into a clean tube. A further 0.5 mL of the lysis solution was added and the cycles of lysis were repeated, adding the new supernatant to the former. This soluble fraction was centrifuged at 1,500 g for 5 min, collected and then centrifuged at 16,000 g for 15 min. The microsomal fraction was precipitated at 22,000 g for 2 h and it was then resuspended in 50 μL 100 mM phosphate buffer [pH 7.5] for immediate use. All the fractionation steps were carried out at 0-4 ºC.

2.8. GPAT assay

GPAT activity was measured on microsomes of *gat1Δ* transformants using a modification of the protocol reported by Ruiz-Lopez *et al.* [12]. The incubation mixture (final volume of 100 μL) contained 50 mM bis-tris propane [pH 7.0], 1.5 mM G3P (Sigma-Aldrich), including 3,700 Bq L-[U-^{14}C]glycerol-3-phosphate (American Radiolabeled Chemicals, St Louise, MO, USA), 0.3 mM acyl-CoA (Sigma-Aldrich) and 0.05 % (w/v) BSA. The reaction was started with the addition of 50 μg of microsomal proteins and it ran for 15 min at 30 ºC unless otherwise specified. The reactions were stopped by adding 100 μL of 0.15 M acetic acid and the lipids were extracted and analyzed as described originally.

2.9. LPAAT assay

LPAAT activity was measured on microsomes isolated from *ale1Δ* transformants. The reaction mixture (a final volume of 100 μL) contained 100 mM phosphate buffer [pH 7.5], 50 μM 1-oleoyl [1-oleoyl-9,10-^{3}H]LPA (3,667 Bq) (Perkin Elmer, Waltham, MA, USA), 20 μM acyl-CoA (Sigma-Aldrich), 1 mM $MgCl_2$, 1 mM DTT and 50 μg of microsomal proteins. After incubating at 30 °C for 5 min, the reactions were stopped by adding 100 μL 0.15 M acetic acid, and the lipids were extracted by adding a further 500 μL of chloroform/methanol (1:1, v/v) followed by gentle mixing and spinning at 2,000 g for 10 min. The lower chloroform phase containing the extracted lipids was recovered and the aqueous phase was re-extracted with a further 250 μL of chloroform. The lower phase recovered was combined with that previously extracted, it was evaporated under nitrogen at 36 °C and reconstituted in 50 μL of the chloroform/methanol mixture (2:1, v/v). Subsequently, 25 μL of the lipid suspension was analyzed by thin layer chromatography, as described by Ruiz-Lopez *et al*. [12], and the remaining volume was quantified on an Ecoscint scintillant (National Diagnostics, Atlanta, GA, USA) and with a LS-6500 Multipurpose Scintillation Counter (Beckman Coulter, Brea, CA, USA).

3. Results

3.1. Cloning of two sunflower GPAT genes: a phylogenetic study

Based on the sequences of previously described microsomal GPAT3 from mouse and GPAT9 from *Arabidopsis*, we performed a sequence homology search of ESTs in *Helianthus* species, identifying fragments of two putative GPAT genes. The coding sequences for these two isoforms were successfully amplified from sunflower seed cDNA and they encoded proteins of 371 amino acids with a predicted molecular weight of 42.6 kDa. Blast searches at the nucleotide level using each isoform as a query against closely related species in the Asterid subclass only yielded results for isoform 2 (data not shown). Even though sunflower behaves as a diploid, the presence of two isoforms is probably due to the ancestral polyploid origin of the *Helianthus* genus [31]. Also, more than one isoform was observed in other hybrid or polyploid species (e.g., *Malus* x *domestica*, *Sesamum indicum*, *Glycine max*: Fig. 1).

Comparison of these *Ha*GPAT9 proteins with other similar proteins revealed 75-90% identity with those from flowering plants, 45-70% with those from more distant Viridiplantae species and 25-35% identity with similar GPAT proteins in animals. Protein alignment across various kingdoms revealed that 18% of the residues were identical (Fig. S2). Clustering of homologous GPAT proteins yielded a tree consistent with the taxonomic relationships among their source species (Fig. 1), a tree that

was rooted using a couple of LPAAT proteins from *A. thaliana* as the outgroup. All sequences belonging to Viridiplantae species clustered well together (88% bootstrap), while separate clades contained the rest of the taxonomic groups (rhodophyta, amoebozoa, opisthokonta and vertebrates). The two sunflower isoforms are grouped together in a same clade.

3.2. Proteomic analysis of seed microsomes

In this study, sunflower seed microsomal proteins were analyzed using a combination of one-dimensional gel electrophoresis followed by liquid chromatography-mass spectrometry. The sample complexity was reduced by SDS-PAGE pre-fractioning prior to trypsin digestion (Fig. S1). In addition to the sunflower sequences contained in the online databases, known sequences for acyltransferases were included in the main search database and they were also used to generate a specific database for post-translational modifications.

After applying a 1% false discovery rate (FDR) cut-off, this approach resulted in the identification of 4,413 non-redundant peptides representing 991 proteins. From these, the product of the *HaGPAT9-1* gene (GenBank accession EF552845) was the most noteworthy. The corresponding peptides were derived from the SDS-PAGE band containing proteins in the range of 35-40 kDa (Fig. S1).

A further search against a custom database containing sunflower acyltransferase sequences was carried out to find peptides with post-translational modifications. This search revealed the presence of four *Ha*GPAT9-1 peptides defined by 7 spectra (Table 2). Of these, two peptides were unmodified, one was carbamidomethylated and the other contained two phosphorylated residues (Tyr21 and Thr32). The Tyr21 residue is conserved among all the flowering plant species analyzed (Fig. S2), whereas Thr32 was only found in isoform 1. No deamidated peptides were found.

3.3. Evaluation of the relevant proteins in sunflower microsomes

The assignment of GO terms to the proteins revealed that most of the involved biological processes were related to protein and nucleic acid metabolism (Table S3). 39 sequences were associated to lipid metabolic process (GO: 0006629); at least 20 of them participate in *de novo* lipid biosynthetic pathways and 7 in lipid degradation (Table 3). Amongst the enzymes involved in lipid synthesis that were associated with the ER, two long chain acyl-CoA synthetases were found, as well as a delta-12 oleate desaturase and a phosphatidylcholine:diacylglycerol acyltransferase (PDAT). There was a large representation of soluble proteins related with intraplastidial fatty acid biosynthesis, including: acetyl-CoA carboxylase

subunits, malonyl-CoA:ACP transacylase, components of the fatty acid synthase complexes, acyl-ACP thioesterases and stearoyl-ACP desaturases. Moreover, many proteins involved in lipid degradation and β-oxidation were also present in this fraction, such as an acyl-CoA synthetase, a delta(3,5)-delta(2,4)-dienoyl-CoA isomerase, acyl-CoA oxidases and 3-hydroxyacyl-CoA dehydrogenases (Table 3). A large number of the identified spectra belonged to proteins implicated in protein metabolism (Table S2). Moreover, 11S globulin seed storage proteins were also detected due to the pH conditions used for precipitation in the preparation of the microsomes [32].

3.4. Subcellular localization of HaGPAT9-1

The subcellular localization of *Ha*GPAT9-1 was studied in tobacco BY-2 cells by confocal microscopy [33, 34, 35]. The transient expression of *Ha*GPAT9-1-GFP (via biolistic bombardment) in an individual BY-2 cell revealed a reticular distribution that was similar to the fluorescence attributable to the ER marker ConA, indicating that *Ha*GPAT9-1 is an ER resident protein (Fig. 2, top row). Closer inspection of the images revealed that the distribution of the GFP-tagged protein was not entirely uniform throughout the ConA-stained ER but rather, it was at times enriched in distinct regions of the ER or, less frequently, localized to regions that were devoid of ConA (Fig. 2, bottom row; see solid and open arrowheads). The

presence of aggregated ER structures was also conspicuous in *Ha*GPAT9-1-GFP-transformed cells (Fig. 2, top row). Similar alterations in ER morphology were not detected in neighboring untransformed BY-2 cells, yet they have been reported in plant cells ectopically expressing other GPATs or other lipid biosynthetic enzymes [36, 37, 38, 7], suggesting that they are a consequence of altering the amount of lipids in the ER membrane.

3.5. Functional complementation assay in yeast

An assay of GPAT activity based on the complementation of the cmy228 *S. cerevisiae* strain (Table 1) was designed to evaluate the *in vivo* functionality of the *Ha*GPAT9 proteins identified (Fig. 3). Yeasts possess two GPAT genes, *GAT1* and *GAT2*, and disrupting either of these alone does not cause detectable growth effects. By contrast, disruption of both genes together is lethal. The yeast cmy228 strain is *gat1Δgat2Δ* and it contains the vector p*GAL1*(*URA3*)::*GAT1* that drives galactose inducible expression of *GAT1*, allowing these cells to survive in the presence of this substrate. To determine whether the activity of either of the sunflower GPATs could replace the missing activity in this yeast mutant, they were introduced into an expression system under the regulatory control of the constitutive GPD promoter (p416[*LEU2*]::*HaGPAT9-1* and *2*) and used to transform cmy288 strain. The prototrophic strain S288C and the

auxotrophic strain W303-1A carrying the empty p416(*LEU2*) vector were used as URA+ and URA- controls, respectively.

The strains grown under control conditions of plasmid selection and induction (Fig. 3A) behaved quite distinctly to those grown on glucose, where the lethal phenotype of the cmy288 strain (Fig. 3B) was overcome by expressing the product of *HaGPAT9-1* gene. However, the application of 5-fluoroorotic acid (FOA) to URA supplemented medium, which is lethal for URA+ cells, inhibited the growth of any cell that had not lost the pGAL1 plasmid (Fig. 3C). Therefore, the *Ha*GPAT9 does not fully complement yeast GAT functionality. Growth in media not selecting p416 (Fig. 3D) triggered the loss of such plasmids carrying the heterologous enzymes, decreasing the rate at which cells grew (compare with Fig. 3B).

3.6. Overexpression of sunflower GPAT9s modifies the TAG profile in yeast

A second approach to indirectly investigate the enzymatic activity of *Ha*GPAT9s was to analyze the modifications induced in yeast TAGs. Sunflower GPAT coding sequences were introduced into the inducible pYES2 expression vector, which was transformed into the GPAT deficient *gat1Δ* yeast strain. After growth on selective and inducible media the yeast cells were harvested, dried and weighted, and their TAGs extracted,

analyzing both the TAG profile on a mass spectrometer and the TAG fatty acid composition.

After normalization of the TAG data with internal lipid standards and according to samples dry weight, the over-expression of both heterologous enzymes revealed an increase in the total amount of TAGs produced by the transformants relative to the controls (Fig. 4). *Ha*GPAT9-1 expression induced the accumulation of most TAG species, a composition not displayed by its counterpart. The most abundant TAG species contained either 48 or 50 carbon atoms. Regarding the degree of unsaturation, TAGs containing less than C48 were present in saturated species, although there was a preference to contain one unsaturated fatty acid, whereas longer TAGs possessed at least one unsaturated fatty acid. Additionally, the differences in the accumulation of TAG species were consistent with the fatty acid composition of TAGs in the three strains (Fig. 5).

3.7. Glycerol-3-phosphate and lysophosphatidate acyltransferase activities of the HaGPAT9 proteins

The GPAT assays carried out on microsomal preparations of the *gat1Δ* yeast strain carrying the empty plasmid (control cells) displayed reduced background activity. After over-expressing both sunflower isoforms, only the construct carrying *HaGPAT9-1* induced an increase in GPAT activity. The influence of reaction time was evaluated by running the assays for 15

or 30 min (Fig. 6A) and as the activity was 60% higher after the shorter 15 min reaction time, this was used in the following assays. The substrate specificity was investigated using different acyl-CoA derivatives and the strongest activity was evident with 16:0-CoA, followed by 18:2-CoA and 18:1-CoA (Fig. 6B). Compared to control, activity of yeast expressing *Ha*GPAT9-1 with 16:0-CoA experienced a two-fold significant increase while it raised to three-fold with the unsaturated substrates. Only weak activity was displayed towards 18:0-CoA, close to the limits of detection. No activity was detected for *Ha*GPAT9-2 isoform.

The LPAAT activity of GPATs was also evaluated using 1-oleoyl lysophosphatidic acid as the acceptor and different acyl-CoAs. In most cases the expression of the GPATs in yeast did not significantly increase the background LPAAT activity of the yeast microsomes (Fig. 6C), and a small but a significant increase in LPAAT activity was only measured when *Ha*GPAT9-1 was expressed and 18:1-CoA or 18:2-CoA were the acyl donors. By contrast, the LPAAT activity associated with expression of the second isoform was lower than that of the controls.

3.8. HaGPAT9 expression

The expression of microsomal GPATs was studied in developing sunflower seeds and vegetative tissues by RT-qPCR. *HaGPAT9-1* is more actively transcribed than its homologue in most of the tissues analyzed

(Fig. 7A), and the expression of this isoform was upregulated at the initial phases of embryo development and at the late stage of seed maturation. In addition, this isoform was strongly expressed in leaves. The *HaGPAT9-2* gene exhibited a very different profile and it was generally expressed more weakly than its homologue. This isoform was only upregulated at early and mid-stages of seed development, as well as in vegetative tissues.

4. Discussion

TAGs accumulate during sunflower seed maturation to reach values up to 40-50% of the total seed weight. The first acylation reaction to produce these TAGs is carried out by *sn*-1 GPAT enzymes although in an initial search no such candidate proteins were identified in sunflower [12]. Later, 60 Kd sunflower GPATs were detected that were associated to a plant specific *sn*-2 GPAT family, GPATs 1-8 in Arabidopsis, involved in cutin/suberin biosynthesis [5]. No GPAT from this family was identified in our mass spectrometry analysis. A protein recently associated with TAG biosynthesis is the *Arabidopsis* GPAT9 [7, 8] and here, we provide an extensive characterization of its counterpart in sunflower.

We have cloned two GPAT genes from developing sunflower seeds designated *HaGPAT9-1* and *2* after the *Arabidopsis* gene. Isoform 1 was the enzyme identified by proteomics in the membranes of embryos at the onset of the oil accumulation. This isoform contains some conserved blocks when aligned with homologous proteins, indicating the probable fragments that define the active site (e.g., the HX_4D motif present in many acyltransferases) [39] and substrate binding regions (Fig. S2). However, examination of their amino acid sequences showed the changes both sunflower isoforms accumulate in relation to their homologues.

A phylogenetic study showed a broad spectrum of taxonomic groups that have proteins similar to this GPAT, suggesting an ancient

origin (at least in early eukaryotes) before they evolved into the current kingdoms. The disposition of clades in the tree is coherent with the group taxonomy, as partially reflected in the plant clade. Investigation of the genome evolution in those plant species carrying multiple isoforms of this enzyme points to hybridization and changes in ploidy as the probable sources of the duplications. In view of our results, multiple isoforms do not appear to imply enzyme redundancy. In this regard, the presence of multiple GPAT proteins is frequent in nature, with the most representative example of multiple gene duplication and functional diversification depicted by the Arabidopsis GPAT1-8 family [5]. Conversely, GPAT9 has a single functional isoform, recently revealed by mutant analysis [8]. It is noteworthy that some eukaryotic clades do not contain any GPAT9 homologues, the most relevant belonging to Fungi kingdom. A Blast search only returned a few sequences sharing moderate similarity, none of which belonged to the yeast Dikarya sub-kingdom (Fig. S3). Instead, yeast enzymes with GPAT activity, Gat1p and Gat2p [16], are more similar to a plant GPAT family involved in polyester synthesis [40]. Furthermore, they not only possess GPAT but also dihydroxyacetone phosphate acyltransferase (DHAPAT) activity, improving their functionality. In general, GPATs exhibit a high degree of redundancy, not only due to the presence of GPAT activity in various protein families but also, due to the multiplication and evolution of distinct family members. The fungal case is

a clear example of how the redundant GPAT activity present in most organisms produces viable organisms with improved competitive capacity even after the loss of one isoform.

To identify GPATs involved in lipid biosynthesis and considering that these acyltransferases are membrane bound proteins, membrane protein fractions from developing sunflower seeds (15 DAF) were analyzed by mass spectrometry. The only GPAT protein found in this fraction was *Ha*GPAT9-1 (GenBank accession EF552845), which was unequivocally identified as the peptides detected accounted for 68 of the 371 amino acids of the full length sequence (18% coverage). Moreover, all them corresponded to the *Ha*GPAT9-1 isoform despite the high similarity with its close homologue *Ha*GPAT9-2 (90% amino acid identity, GenBank accession EF552846). Phosphoresidue analysis revealed the presence of a peptide with two phosphorylated sites at the N-terminus of the protein (Tyr21 and Thr32), suggesting that its enzyme activity or subcellular localization could be modified by specific kinases. The Tyr21 residue is conserved among the homologues in all the flowering plant species analyzed, suggesting a regulatory role of this amino acid. By contrast, Thr32 is unique to *Ha*GPAT9-1 and its function is not yet known. Interestingly, the Gly32 residue in *Ha*GPAT9-2 is also highly conserved in other homologues, suggesting functional divergence in the regulation of the two *Ha*GPAT9 isoforms. The activity of yeast GPATs is regulated post-

translationally by phosphorylation of the C-terminus, although it is not clear whether phosphorylation regulates GPAT localization [41]. Our results support the potential phosphorylation of *Ha*GPAT9-1 under physiological conditions, suggesting an analogous regulatory mechanism.

At 15 DAF, both embryo growth and the accumulation of storage oil by the seed are very active, as reflected by the complexity of the enzymes determined by mass spectrometry that are involved in biological functions like protein synthesis and fate, metabolism and energy. The proteomic analysis of sunflower seed membranes identified enzymes related to lipid metabolism other than GPATs. For example, the identified PDAT belongs to an alternative pathway of TAG biosynthesis that involve the transesterification of phosphatidylcholine (PC) and diacylglycerol (DAG) to yield lyso-PC and TAG. Previous research demonstrated that both diacylglycerol acyltransferase (DAGAT) and PDAT contribute to TAG synthesis in sunflower seeds, and although DAGAT is more active, it has a lower substrate affinity than PDAT [42]. Our finding highlights the interest on this alternative pathway for TAG synthesis. Nonetheless, identification of other enzymes in the Kennedy pathway, LPAAT and DAGAT, is still missing.

Considering that the method used to obtain the microsomal fraction did not exclude organelle membranes, the proteins detected were from various subcellular localizations. Thus, many soluble enzymes related to

fatty acid synthesis were found, such as the stearoyl-ACP desaturase that was among the most abundant proteins in the microsomal fraction (Table S2) and that is strongly expressed in sunflower embryos [13]. Also, the first step in fatty acid synthesis is represented by the alpha subunit of the acetyl-CoA carboxylase complex (sunflower EST GE494904). However, not only enzymes related to lipid biosynthesis were sequenced in microsomes but also those involved in beta-oxidation, suggesting the development of peroxisomes for eventual seed germination. Despite the good coverage of the activities in the lipid biosynthesis pathway, this method did not capture proteins represented by enzymes either at a low abundance or for which sequences have not yet been cloned in *H. annuus*.

The *Ha*GPAT9-1 enzyme was clearly located in the ER and based on the variation in fluorescence intensity, this enzyme is more abundant in the perinuclear ER than in the cortical membrane when over-expressed in tobacco cells. Moreover, the ER morphology of cells producing the heterologous protein is altered, forming membrane aggregates in accordance with the altered ER morphology in cells expressing mammalian GPAT3 [43] or *A. thaliana* GPAT9, and even GPAT8 [7]. Similar results were obtained after overexpression of a human LPAAT [44]. Also, the accumulation of lipid intermediates may recruit interactors by generating microdomains [45]. Then, the prominent globular ER structure is probably formed due to: (i) the accumulation of a high proportion of

acyltransferases; (ii) their activity altering the membrane properties; and/or (iii), the increase in membrane destabilizing lipids. Moreover, the recurrent alteration of the ER after an enrichment of acyltransferase activity also suggests the regulated formation of a possible lipogenetic structure.

In vivo functional assays were based on the complementation of lethality that the disruption of both yeast *GAT* genes causes in the cmy228 strain. Constitutive expression of *HaGPAT9-1* allowed yeast to grow without inducing *GAT1* expression. Full complementation would have allowed yeast cells to lose the pGAL1(*URA3*) plasmid carrying *GAT1* and then grow under FOA negative selection. As indicated above, yeast GPATs belong to a different GPAT family and they exhibit GPAT/DHAPAT activities. Thus, *Ha*GPAT9-1 activity complements the cmy228 strain under certain growth conditions, although GPAT alone does not allow cell survival. Nevertheless, this study reveals that *HaGPAT9-1* encodes an enzyme with GPAT activity while that of its counterpart could not be determined. The TAG content and composition in yeast was also altered when sunflower GPATs were expressed, reflected by an increase in the total amount of TAGs as well as an enrichment in 16:0 and 16:1 fatty acids. Hence, both enzymes are active in the yeast heterologous system and their consequences are reflected in the alteration of yeast lipids. In this regard, the significant modifications detected in the strain over-expressing *Ha*GPAT9-1 suggest enzyme selectivity towards saturated fatty acids. On

the contrary, the *Ha*GPAT9-2 enzyme does not change the TAG composition.

GPAT *in vitro* selectivity was studied in microsomal fractions from a yeast strain with reduced GPAT activity, the *gat1Δ* mutant. Microsomes were incubated with radiolabeled G3P and different acyl-CoAs, and the products were a mixture of LPA combined with lipids derived from this in the downstream TAG biosynthetic pathway. Thus, the total radioactivity in the products of LPA, phosphatidic acid (PA), diacylglycerol (DAG) and TAG were quantified. Accordingly, only *Ha*GPAT9-1 activity was detected *in vitro*, with high specificity towards 16:0-CoA and 18:2-CoA, lower specificity towards 18:1-CoA and very low for 18:0-CoA. This activity is consistent with previous measurements of GPAT activity in sunflower seed microsomes [12] and with the TAG composition of sunflower, a species in which palmitic acid predominates at the *sn*-1 position. The high GPAT specificity towards palmitoyl-CoA is also consistent with the increase in TAG species with a palmitoyl moiety at the *sn*-1 position in yeasts transformed with *Ha*GPAT9-1.

In light of the conservation of sequence motifs among acyltransferases, the *Ha*GPAT9s were tested for LPAAT activity. Indeed, the length of these enzymes is similar to that of plant LPAATs, much shorter than the plant GPATs characterized [5]. We used the *ale1Δ* mutant reduced in lysophospholipid acyltransferase activity as the host strain in

these assays. *Ha*GPAT9-1 strain had weak yet significant LPAAT activity with oleoyl- and linoleoyl-CoA substrates. However, direct implication of *Ha*GPAT9-1 to the change in LPAAT activity could not be verified. Interestingly, the LPAAT activity of membranes carrying *Ha*GPAT9-2 was significantly reduced with the stearoyl-CoA substrate. Thus, although the isoform 2 did not utilize G3P or *sn*-1-LPA as acyl acceptors, it is an enzyme that potentially competes for acyl-CoA substrates in a yet unknown mechanism. Our results are in agreement with the enzyme activity in microsomes from developing siliques of *Arabidopsis GPAT9* knock-down line [8], which was reduced in GPAT activity but not LPAAT activity.

*Ha*GPAT9-1 is strongly expressed at the onset of TAG accumulation in seeds and leaves; the pattern observed during seed filling responds to the variations on the oil accumulation rate described previously [46], suggesting that *Ha*GPAT9-1 is involved in oil deposition in sunflower seeds. By contrast, *Ha*GPAT9-2 was strongly expressed in vegetative tissues with only short periods of activation in oil accumulating seeds. The first upregulation at 12 DAF coincides with the end of the pericarp growth period while a second upregulation at 21 DAF occurs when the embryo is actively developing [47]. This differs from the Arabidopsis GPAT9 transcripts [48] that remain at similar levels in all the represented tissues and that are slightly downregulated at early stages of

embryo development, suggesting constitutive expression of this gene. Also, a GPAT9-like transcript was found by RNA-sequencing of castor bean (*Ricinus communis*) that is expressed in all tissues, and especially in the developing seed endosperm [49], being the most abundant GPAT transcripts in the endosperm. The analysis of the sunflower genes performed here suggests that *Ha*GPAT9-1, which is present in all tissues, carries the ancestral GPAT9 activity, and there is certain a functional divergence in this species revealed by the activity of *Ha*GPAT9-2.

Supplementary Data

Supplementary data are available at Plant Science online.

Funding

This work was supported by the "Ministerio de Economia y Competitividad" and FEDER [AGL2014-53537-R and JAE-CSIC to M.P-M].

Acknowledgments

We thank A. González-Callejas and B. Lopez-Cordero for their skillful technical assistance. We also thank Dr Ana Rincón for kindly providing the p416(*LEU*) plasmid.

References

[1] M. Frentzen, Acyltransferases and triacylglycerols, in: TSMJ (Eds.), Lipid Metabolism in Plants, CRC Press, Boca Raton, 1993, pp. 195–220.

[2] M. Bafor, L Jonsson, AK Stobart, S Stymne S, Regulation of triacylglycerol biosynthesis in embryos and microsomal preparations from the developing seeds of *Cuphea lanceolate*, Biochemical Journal 272 (1990) 31-38.

[3] E.P. Kennedy, S.B. Weiss, The function of cytidine coenzymes in the biosynthesis of phospholipides. The Journal of biological chemistry 222 (1956) 193-214.

[4] SK. Gidda, J.M. Shockey, S.J. Rothstein, J.M. Dyer JM, R.T. Mullen, *Arabidopsis thaliana* GPAT8 and GPAT9 are localized to the ER and possess distinct ER retrieval signals: functional divergence of the dilysine ER retrieval motif in plant cells, Plant Physiology and Biochemistry 47 (2009) 867-879.

[5] W. Yang, J.P. Simpson, Y. Li-Beisson, F. Beisson, M. Pollard, J.B. Ohlrogge, A land-plant-specific glycerol-3-phosphate acyltransferase family in *Arabidopsis*: substrate specificity, *sn*-2 preference, and evolution, Plant Physiology 160 (2012) 638-652.

[6] M. Payá-Milans, M. Venegas-Calerón, J.J. Salas, R. Garcés, E. Martínez-Force, Cloning, heterologous expression and biochemical

characterization of plastidial *sn*-glycerol-3-phosphate acyltransferase from *Helianthus annuus*, Phytochemistry 111 (2015) 27-36.

[7] S.K. Gidda, J.M. Shockey, S.J. Rothstein, J.M. Dyer, R.T. Mullen, *Arabidopsis thaliana* GPAT8 and GPAT9 are localized to the ER and possess distinct ER retrieval signals: functional divergence of the dilysine ER retrieval motif in plant cells, Plant Physiology and Biochemistry 47 (2009) 867-879.

[8] J. Shockey, A. Regmi, K. Cotton, N. Adhikari, J. Browse, P.D. Bates, Identification of *Arabidopsis* GPAT9 (At5g60620) as an Essential Gene Involved in Triacylglycerol Biosynthesis, Plant Physiology 170 (2016) 163-179.

[9] J. Cao, S. Perez, B. Goodwin, Q. Lin, H. Peng, A. Qadri, Y. Zhou, R.W. Clark, M. Perreault, J.F. Tobin, R.E. Gimeno, Mice deleted for GPAT3 have reduced GPAT activity in white adipose tissue and altered energy and cholesterol homeostasis in diet-induced obesity, American Journal of Physiology - Endocrinology and Metabolism 306 (2014) E1176-1187.

[10] V.S. Eccleston, J.L. Harwood, Solubilisation, partial purification and properties of acyl-CoA: glycerol-3-phosphate acyltransferase from avocado (*Persea americana*) fruit mesocarp, Biochimica et Biophysica Acta 1257 (1995) 1-10.

[11] A.M. Manaf, J.L. Harwood, Purification and characterisation of acyl-CoA: glycerol 3-phosphate acyltransferase from oil palm (*Elaeis guineensis*) tissues, Planta 210 (2000) 318-328.

[12] N. Ruiz-Lopez, R. Garcés, J.L. Harwood, E. Martínez-Force, Characterization and partial purification of acyl-CoA:glycerol 3-phosphate acyltransferase from sunflower (*Helianthus annuus* L.) developing seeds, Plant Physiology and Biochemistry 48 (2010) 73-80.

[13] J.J. Salas, E. Martínez-Force, R. Garcés, Biochemical characterization of a high-palmitoleic acid *Helianthus annuus* mutant, Plant Physiology and Biochemistry 42 (2004) 373-381.

[14] R.K. Mortimer, J.R. Johnston, Genealogy of principal strains of the yeast genetic stock center, Genetics 113 (1986) 35-43.

[15] B.J. Thomas, R. Rothstein, Elevated recombination rates in transcriptionally active DNA, Cell 56 (1989) 619-630.

[16] S.A. Minskoff, P.V. Racenis, J. Granger, L. Larkins, A.K. Hajra, M.L. Greenberg, Regulation of phosphatidic acid biosynthetic enzymes in *Saccharomyces cerevisiae,* The Journal of Lipid Research 35 (1994) 2254-2262.

[17] K. Hofmann, A superfamily of membrane-bound O-acyltransferases with implications for wnt signaling, Trends in Biochemical Sciences 25 (2000) 111-112.

[18] V. Zaremberg, C.R. McMaster, Differential partitioning of lipids metabolized by separate yeast glycerol-3-phosphate acyltransferases reveals that phospholipase D generation of phosphatidic acid mediates sensitivity to choline-containing lysolipids and drugs, The Journal of Biological Chemistry 277 (2002) 39035-39044.

[19] D. Mumberg, R. Muller, M. Funk, Yeast vectors for the controlled expression of heterologous proteins in different genetic backgrounds, Gene 156 (1995) 119-122.

[20] J.P. Simpson, R. Di Leo, P.K. Dhanoa, W.L. Allan, A. Makhmoudova, S.M. Clark, G.J. Hoover, R.T. Mullen, B.J. Shelp, Identification and characterization of a plastid-localized *Arabidopsis* glyoxylate reductase isoform: comparison with a cytosolic isoform and implications for cellular redox homeostasis and aldehyde detoxification, Journal of Experimental Botany 59 (2008) 2545-2554.

[21] D.M. Becker, V. Lundblad, Introduction of DNA into yeast cells, Current Protocols in Molecular Biology Chapter 13, 2001, Unit13.7.

[22] A. Sánchez-García, A.J. Moreno-Pérez, A.M. Muro-Pastor, J.J. Salas, R. Garcés, E. Martínez-Force, Acyl-ACP thioesterases from castor (*Ricinus communis* L.): an enzymatic system appropriate for high rates of oil synthesis and accumulation, Phytochemistry 71 (2010) 860-869.

[23] A.M. Tartakoff, P. Vassalli, Lectin-binding sites as markers of Golgi subcompartments: proximal-to-distal maturation of oligosaccharides, The Journal of Cell Biology 97(1983) 1243-1248.

[24] Y. Xue, J. Ren, X. Gao, C. Jin, L. Wen, X. Yao, GPS 2.0, a tool to predict kinase-specific phosphorylation sites in hierarchy, Molecular & Cellular Proteomics 7 (2008) 1598-1608.

[25] F. Sievers, A. Wilm, D. Dineen, T.J. Gibson, K. Karplus, W. Li, R. Lopez, H. McWilliam, M. Remmert, J. Söding, J.D. Thompson, D.G. Higgins, Fast, scalable generation of high-quality protein multiple sequence alignments using Clustal Omega, Molecular Systems Biology 7 (2011) 539.

[26] H. McWilliam, W. Li, M. Uludag, S. Squizzato, Y.M. Park, N. Buso, A.P. Cowley, R. Lopez, Analysis Tool Web Services from the EMBL-EBI, Nucleic Acids Research 41 (2013) W597-600.

[27] A. Conesa, S. Götz, J.M. García-Gómez, J. Terol, M. Tallón, M. Robles, Blast2go: a universal tool for annotation, visualization and analysis in functional genomics research, Bioinformatics, 21 (2005) 3674-3676.

[28] K. Tamura, D. Peterson, N. Peterson, G. Stecher, M. Nei, S. Kumar, MEGA5: molecular evolutionary genetics analysis using maximum likelihood, evolutionary distance, and maximum parsimony methods, Molecular Biology and Evolution 28 (2011) 2731-2739.

[29] V. Fernández-Moya, E. Martínez-Force, R. Garcés, Identification of triacylglycerol species from high-saturated sunflower (*Helianthus annuus*) mutants, Journal of Agricultural and Food Chemistry 48 (2000) 764-769.

[30] M.L. Hamilton, R.P. Haslam, J.A. Napier, O. Sayanova Metabolic engineering of *Phaeodactylum tricornutum* for the enhanced accumulation of omega-3 long chain polyunsaturated fatty acids, Metabolic Engineering 22 (2014) 3-9.

[31] R.C. Jackson, B.G. Murray, Colchicine induced quadrivalent formation in *Helianthus*: evidence of ancient polyploidy, Theoretical and Applied Genetics 64.3 (1983) 219-222.

[32] V.H. Thanh, K. Shibasaki, Major proteins of soybean seeds. A straightforward fractionation and their characterization, Journal of Agricultural and Food Chemistry 24 (1976) 1117-1121.

[33] F. Brandizzi, S. Hanton, L.L. DaSilva, P. Boevink, D. Evans, K. Oparka, J. Denecke, C. Hawes, ER quality control can lead to retrograde transport from the ER lumen to the cytosol and the nucleoplasm in plants, The Plant Journal 34 (2003) 269-281.

[34] Y. Miao, L. Jiang, Transient expression of fluorescent fusion proteins in protoplasts of suspension cultured cells, Nature Protocols 2 (2007) 2348-2353.

[35] J. Denecke, F. Aniento, L. Frigerio, C. Hawes, I. Hwang, J. Mathur, J.M. Neuhaus, D.G. Robinson, Secretory pathway research: the more experimental systems the better, Plant Cell 24 (2012) 1316-1326.

[36] J.M. Dyer, D.C. Chapital, J.C. Kuan, R.T. Mullen, C. Turner, T.A. McKeon, A.B. Pepperman, Molecular analysis of a bifunctional fatty acid conjugase/desaturase from tung. Implications for the evolution of plant fatty acid diversity, Plant Physiology 130 (2002) 2027-2038.

[37] Y.T. Hwang, S.M. Pelitire, M.P. Henderson, D.W. Andrews, J.M. Dyer, R.T. Mullen Novel targeting signals mediate the sorting of different isoforms of the tail-anchored membrane protein cytochrome b5 to either endoplasmic reticulum or mitochondria, Plant Cell 16 (2004) 3002-3019.

[38] J.M. Shockey, S.K. Gidda, D.C. Chapital, J.C. Kuan, P.K. Dhanoa, J.M. Bland, S.J. Rothstein, R.T. Mullen, J.M. Dyer, Tung tree DGAT1 and DGAT2 have nonredundant functions in triacylglycerol biosynthesis and are localized to different subdomains of the endoplasmic reticulum, Plant Cell 18 (2006) 2294-2313.

[39] T.M. Lewin, P. Wang, R.A. Coleman, Analysis of amino acid motifs diagnostic for the *sn*-glycerol-3-phosphate acyltransferase reaction, Biochemistry 38 (1999) 5764-5771.

[40] Z. Zheng, Q. Xia, M. Dauk, W. Shen, G. Selvaraj, J. Zou, *Arabidopsis* AtGPAT1, a member of the membrane-bound glycerol-3-phosphate

acyltransferase gene family, is essential for tapetum differentiation and male fertility, Plant Cell 15 (2003) 1872-1887.

[41] M.W. Bratschi, D.P. Burrowes, A. Kulaga, J.F. Cheung, A.L. Alvarez, J. Kearley, V. Zaremberg, Glycerol-3-phosphate acyltransferases gat1p and gat2p are microsomal phosphoproteins with differential contributions to polarized cell growth, Eukaryotic Cell 8 (2009) 1184-1196.

[42] W. Banas, A. Sánchez García, A. Banas, S. Stymne S. 2013. Activities of acyl-CoA:diacylglycerol acyltransferase (DGAT) and phospholipid:diacylglycerol acyltransferase (PDAT) in microsomal preparations of developing sunflower and safflower seeds, Planta 237 (2013) 1627-1636.

[43] J. Cao, J.L. Li, D. Li, J.F. Tobin, R.E. Gimeno, Molecular identification of microsomal acyl-CoA:glycerol-3-phosphate acyltransferase, a key enzyme in *de novo* triacylglycerol synthesis, Proceedings of the National Academy of Sciences USA 103 (2006) 19695-19700.

[44] W. Tang, J. Yuan, X. Chen, X. Gu, K. Luo, J. Li, B. Wan, Y. Wang, L. Yu, Identification of a novel human lysophosphatidic acid acyltransferase, LPAAT-theta, which activates mTOR pathway, The Journal of Steroid Biochemistry and Molecular Biology 39 (2006) 626-635.

[45] E.E. Kooijman, V. Chupin, B. de Kruijff, K.N. Burger, Modulation of membrane curvature by phosphatidic acid and lysophosphatidic acid, Traffic 4 (2003) 162-174.

[46] C. Santonoceto, U. Anastasi, E. Riggi, V. Abbate, Accumulation dynamics of dry matter, oil and major fatty acids in sunflower seeds in relation to genotype and water regime, Italian Journal of Agronomy 7 (2003) 3-14.

[47] A.I. Mantese, D. Medan, A.J. Hall, Achene structure, development and lipid accumulation in sunflower cultivars differing in oil content at maturity, Annals of botany 97 (2006) 999-1010.

[48] M. Schmid, T.S. Davison, S.R. Henz, U.J. Pape, M. Demar, M. Vingron, B. Scholkopf, D. Weigel, J.U. Lohmann, A gene expression map of *Arabidopsis thaliana* development, Nature Genetics 37 (2005) 501-506.

[49] A.P. Brown, J.T. Kroon, D. Swarbreck, M. Febrer, T.R. Larson, I.A. Graham, M. Caccamo, A.R. Slabas, Tissue-specific whole transcriptome sequencing in castor, directed at understanding triacylglycerol lipid biosynthetic pathways, PLoS One 7 (2012) e30100.

Figure legends

Fig. 1. Clade representation of proteins homologous to *Ha*GPAT9. Phylogeny reconstruction using the minimum evolution method. Bootstrap values based on 1000 replications are shown at the nodes with values below 50% condensed. Two LPAATs from *Arabidopsis thaliana* were used to root the tree.

Fig. 2. Localization of *Ha*GPAT9-1 to the ER in tobacco BY-2 cells transiently transformed (via biolistic bombardment) with *Ha*GPAT9-1-GFP and stained with the ER marker, ConA. The merged image shows the co-localization of *Ha*GPAT9-1-GFP and ConA at the ER. The asterisk in the merged image highlights a region of aggregated ER. The boxes represent the area of the cell shown at higher magnification in the bottom row. Solid and open arrowheads in the bottom row represent examples where *Ha*GPAT9-1-GFP appears to be localized to distinct regions of the ConA-stained ER and regions devoid of ConA, respectively. Scale bar = 10 μm.

Fig. 3. Complementation assay of the double GPAT cmy228 mutant yeast strain with the two *Ha*GPAT9 isoforms. The strains are displayed in rows and the dilutions in the columns. (A-D) The plate composition is specified at the bottom of each image: A, *S. cerevisiae* strain S288C; B, *S. cerevisiae* strain cmy228 p416(*LEU2*); C, *S. cerevisiae* strain cmy228 p416(*LEU2*)*::HaGPAT9-1*; D, *S. cerevisiae* strain cmy228 p416(*LEU2*)*::HaGPAT9-2*; E, *S. cerevisiae* strain W303-1A p416(*LEU2*).

Fig. 4. TAG molecular species in yeast over-expressing a sunflower *Ha*GPAT9 and the empty vector control. Values are the mean ± SD of three replicates. The asterisks indicate statistically significant differences ($P<0.05$) compared to the control.

Fig. 5. Fatty acid distribution in TAGs of yeast over-expressing a sunflower *Ha*GPAT9 and the empty vector control. Values are the mean ± SD of three replicates. The asterisks indicate statistically significant differences ($P<0.05$) compared to the control.

Fig. 6. GPAT enzyme assays in function of (A) time and (B) acyl-CoA substrate. (C) LPAAT assay as a function of the acyl-CoA substrate. Data are the mean of three replicates with SD error bars. The asterisks indicate statistically significant differences ($P<0.05$) compared to the control.

Fig. 7. Expression of the *HaGPAT9-1* (white columns) and *2* (light grey columns) genes in developing seeds and vegetative tissues of *Helianthus annuus*, and of *GPAT9* from *Arabidopsis thaliana*. (A) Expression in sunflower determined by RT-qPCR: DAF, days after flowering. (B) Expression in *Arabidopsis* from microarrays of Schmid *et al*. [48]. *Arabidopsis* stages: 3, mid globular to early heart embryos; 4, early to late heart embryos; 6, mid to late torpedo embryos; 8, walking-stick to early curled cotyledons embryos; and 10, green cotyledons embryos. The values in panel A represent the mean values ± SD of three independent samples.

Tracked copy

Click here to download E-component(s): ERGPAT reviewed submitted paper tracked.DOCX

Figure 1
Click here to download high resolution image

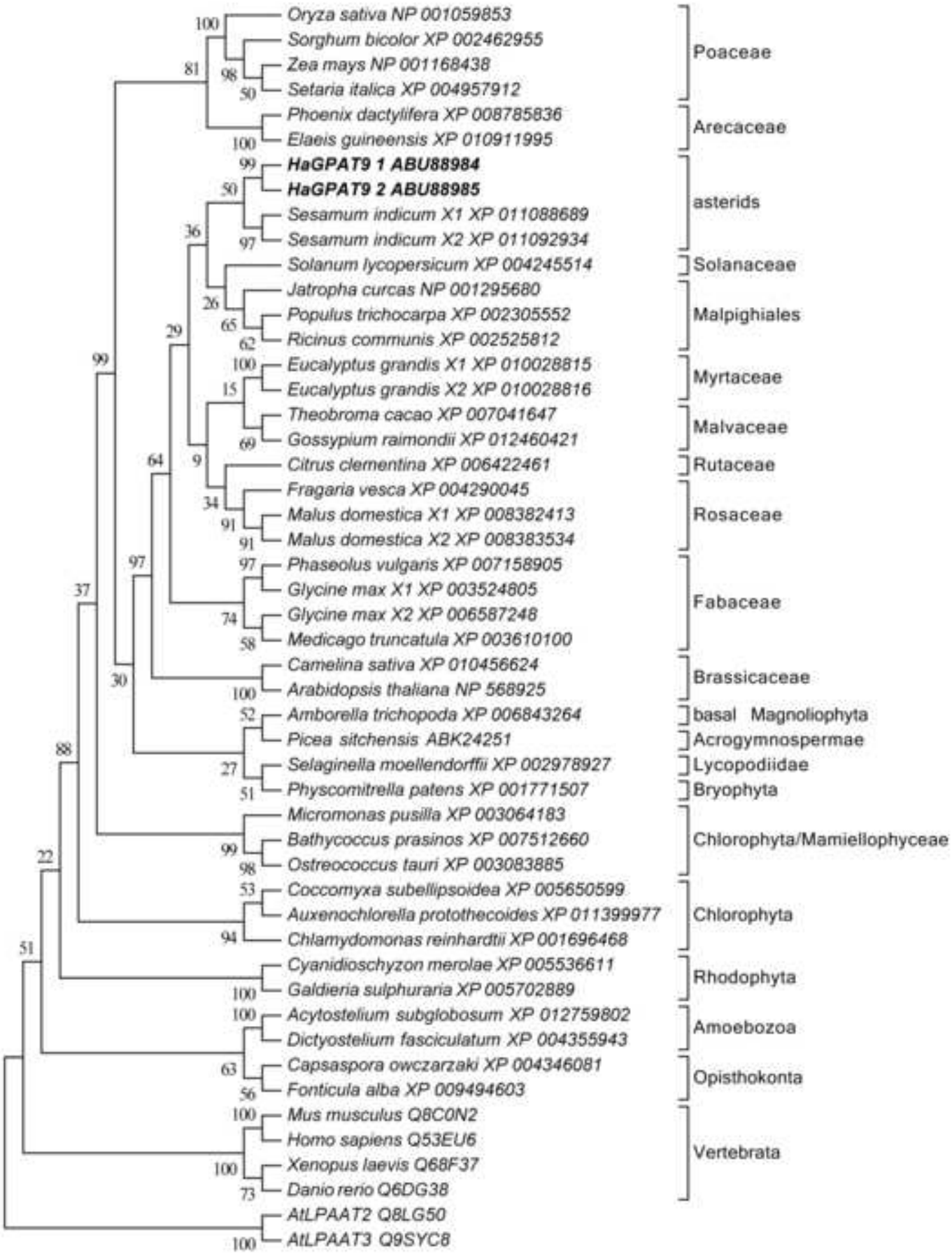

Figure 2
Click here to download high resolution image

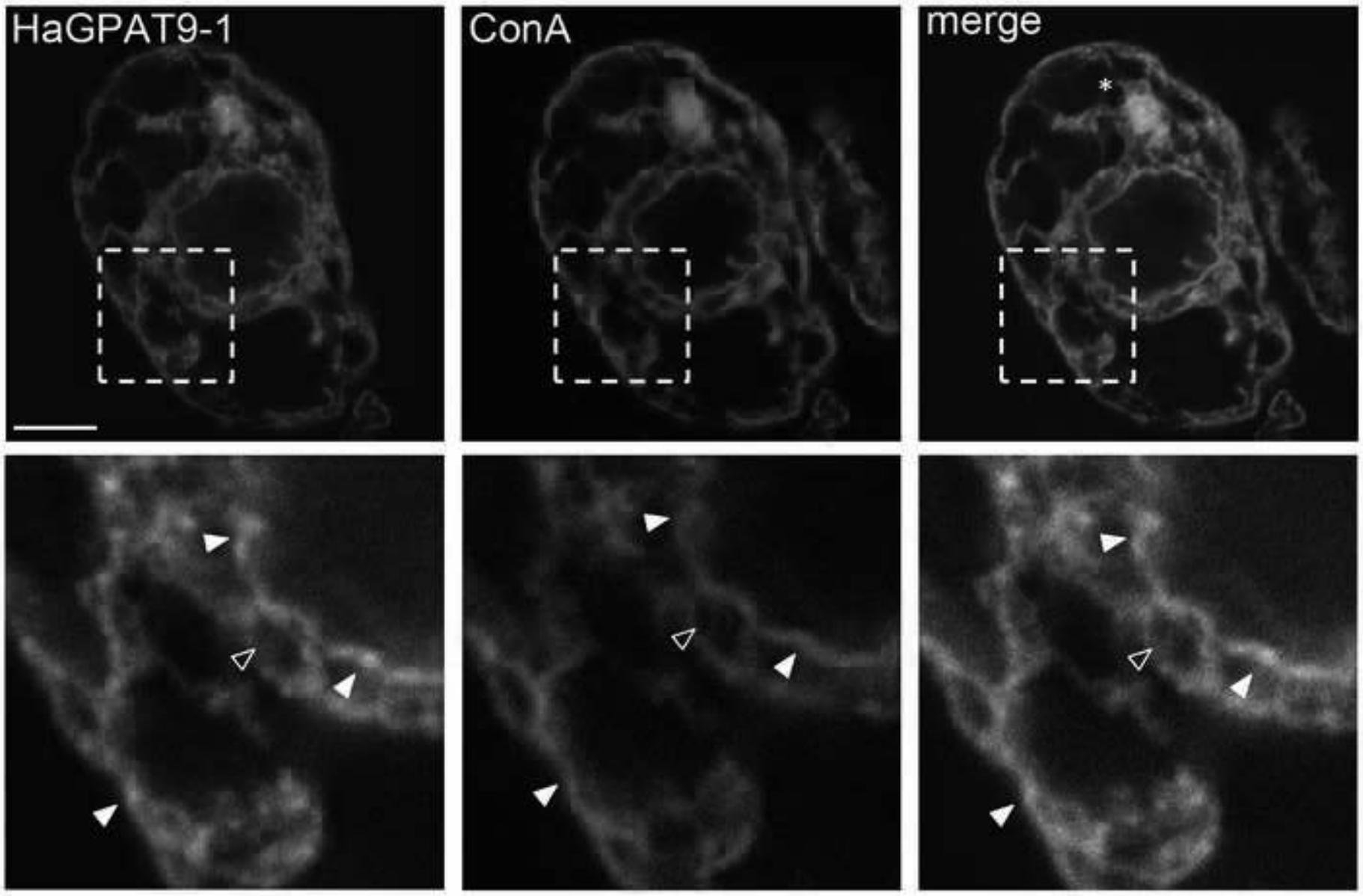

Figure 3

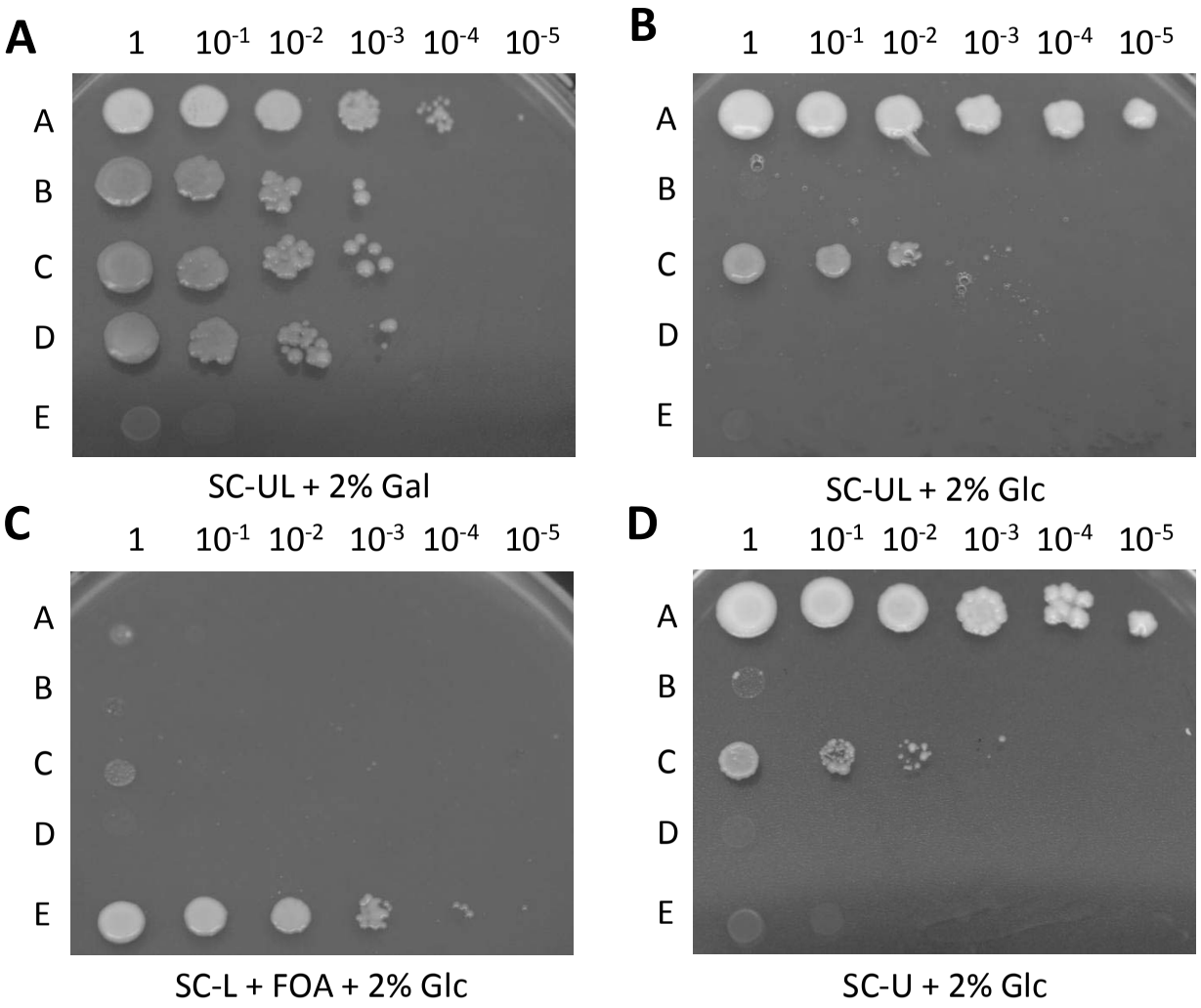
A
1 10-1 10-2 10-3 10-4 10-5
A
B
C
D
E
SC-UL + 2% Gal
B
1 10-1 10-2 10-3 10-4 10-5
A
B
C
D
E
SC-UL + 2% Glc
C
1 10-1 10-2 10-3 10-4 10-5
A
B
C
D
E
SC-L + FOA + 2% Glc
D
1 10-1 10-2 10-3 10-4 10-5
A
B
C
D
E
SC-U + 2% Glc

Figure 4
Click here to download high resolution image

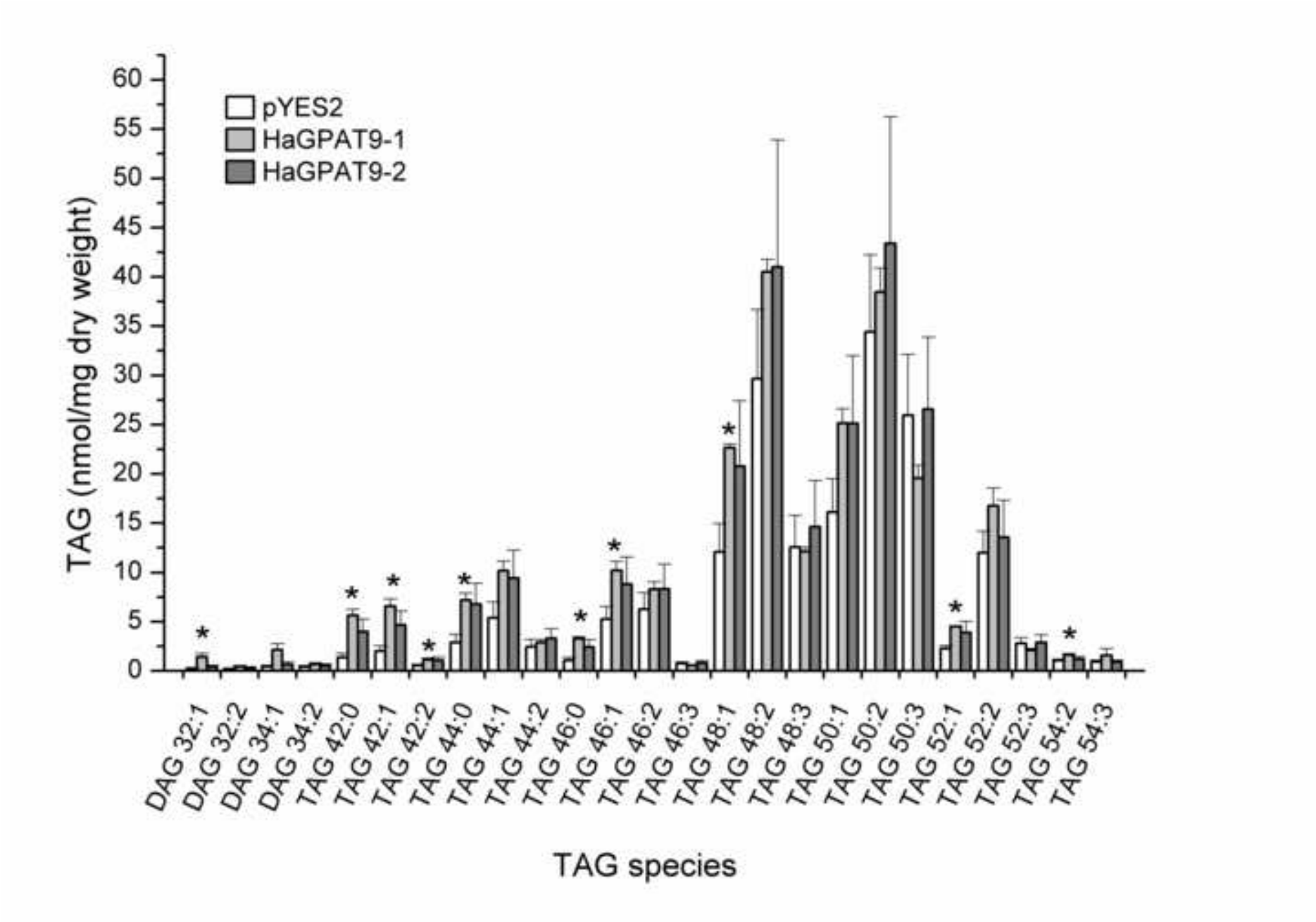

Figure 5
Click here to download high resolution image

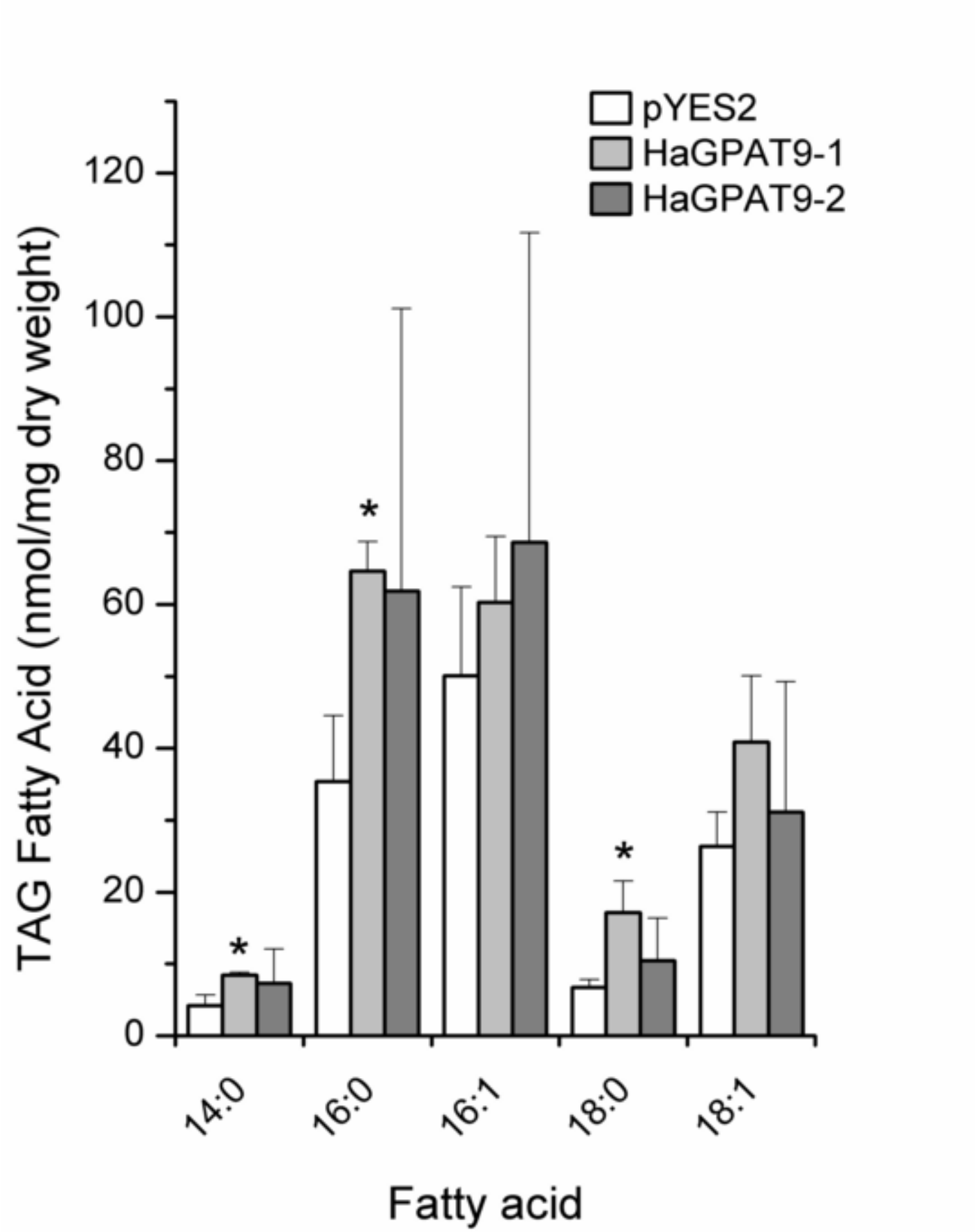

Figure 6
Click here to download high resolution image

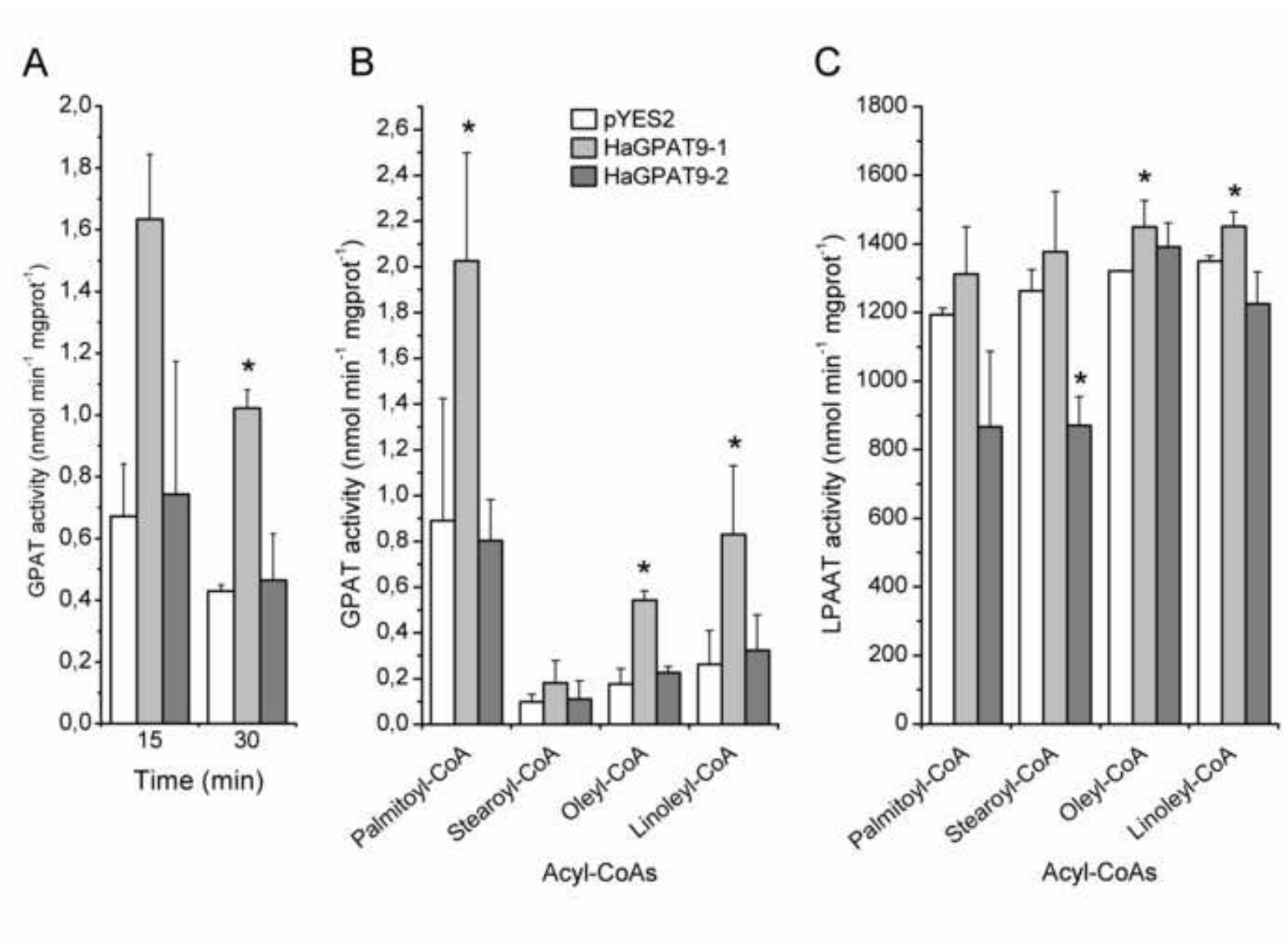

Figure 7
Click here to download high resolution image

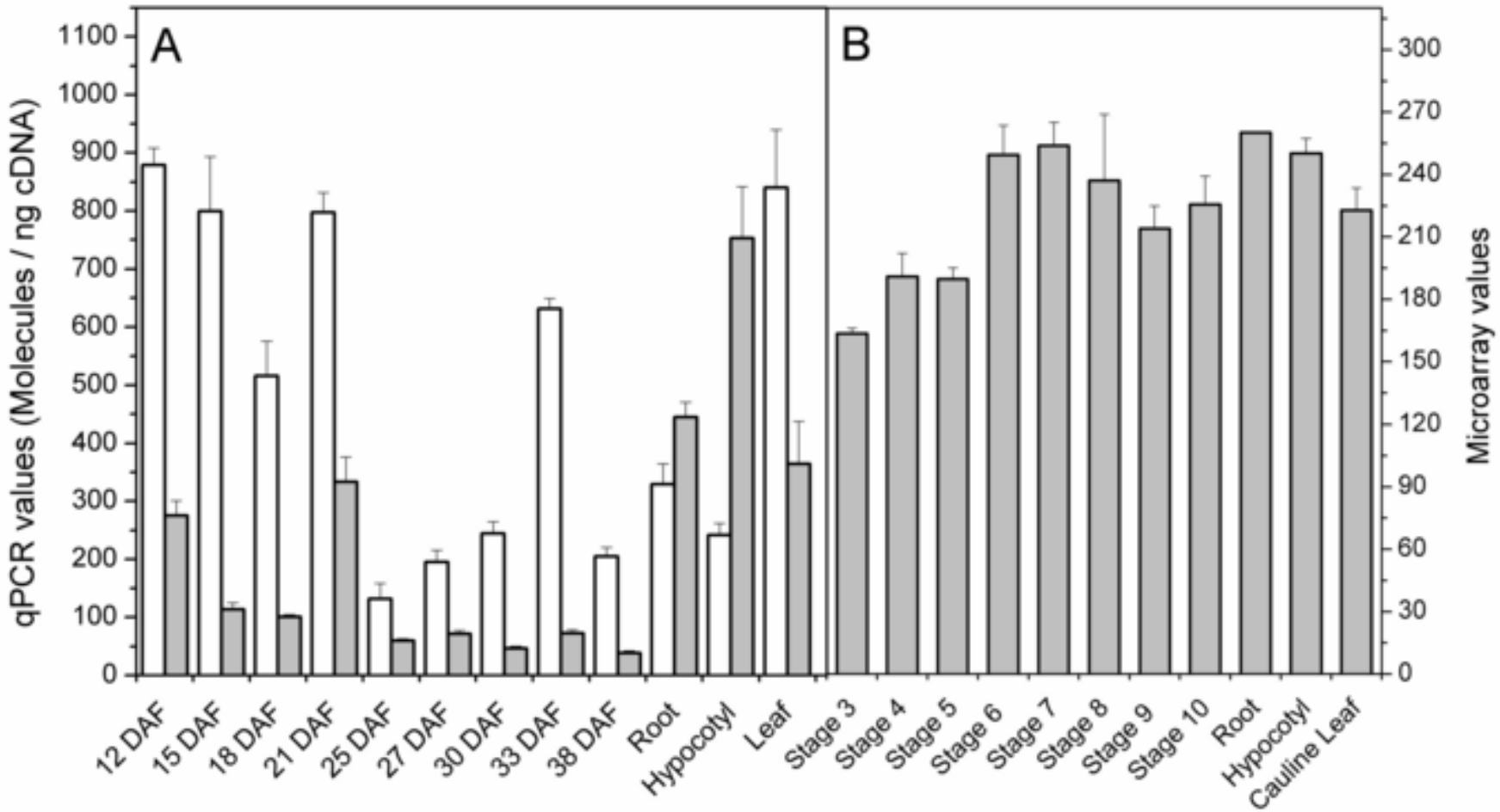

Tables

Table 1. Strains and plasmids used in this study.

Yeast strains and plasmids	**Description**	**Reference or source**
S. cerevisiae		
S288C	MATα SUC2 *gal2 mal2 mel flo1 flo8-1 hap1 ho bio1 bio6*	[14]
W303-1A	MATa {*leu2-3,112 trp1-1 can1-100 ura3-1 ade2-1 his3-11,15*}	[15]
gat1Δ	Mat a; his3D1; leu2D0; lys2D0; ura3D0; YKR067w::kanMX4	[16]
ale1Δ	Mat a; his3D1; leu2D0; met15D0; ura3D0; YOR175c::kanMX4	[17]
cmy228	gat1Δ::TRP1 gat2Δ::HIS3 [pGAL1::*GAT1 URA3*]	[18]
Plasmids		
p416(*LEU2*)	Yeast vector for constitutive expression of proteins under the control of a GPD promoter	[19]
p*GAL1*(*URA3*)::*GAT1*	Plasmid carried by cmy228 that drives galactose inducible expression of *GAT1* to confer viability	[18]
pUC18/NheI-mGFP	pUC18-based expression vector that harbors EmGFP gene driven by the CaMV35S promoter	[20]
pYES2(*URA3*)	Yeast expression vector for native expression of proteins regulated by galactose	Invitrogen

Table 2. The mass spectrometry peptides belonging to the *Ha*GPAT9-1 protein.

Peptide sequence	Best SEQUEST XCorr score	Number of total spectra	Variable modifications identified by spectrum	Charge state
GAFELGATVCPIAIK	2.69	6	c10: Carbamidomethyl (+57.02)	+2H
IFVDAFWNSR	2.05	6		+2H
LRDLLDISPTLTEAAGAIVDDSFTR	2.88	6		+2H
PNIEDYLPPDSIQQPHTK	2.62	1	y6: Phospho (+79.97), t17: Phospho (+79.97)	+3H

Table 3. Proteins in developing sunflower seeds identified by mass spectrometry that are related to lipid metabolism.

Protein	gb	Peptides
Biosynthesis		
Acetyl-CoA carboxylase carboxyltransferase	GE494904	DLYTHLTPIQR, GGVLSHLSPFKPLK, KHEYPWPQDPDPNVK
Malonyl-CoA:acyl carrier protein transacylase	GE514621	GQAMQEAADAAK, LRGQAMQEAADAAK, VPAAAELYNK
Beta-ketoacyl-ACP Synthase III (KAS III)	EF514400	DKMTGLAVEAAQK, ILDAVATRLEIPADR, IVDTSDEWISVR, LEVSNDDLSK, MTGLAVEAAQK, NVLVIGADALSR
Ketoacyl-ACP Synthase III (KAS III)	GE514912	ILTGNESLTGLAAEASLK, IVDTNDEWISAR
Ketoacyl-ACP reductase 1	ADV16374	GITANAIAPGFISSDMTAK, LGEDIEKNILK
Beta-hydroxyacyl-ACP dehydratase	ADE06392	ENFVFAGVDK, ENFVFAGVDKVR, KPVVAGDTLVMR
Beta-hydroxyacyl-ACP dehydratase	ADL60215	DNFFFAGIDK, FPAFPTVIDINQIR, FPFLLVDR, VIEYNPGVSAVAIK
Enoyl-ACP reductase 2	HM021138	AFIAGIADDNGYGWAIAK, AVSASSDTKPLPGLPVDLR
Beta-ketoacyl-ACP synthase (KAS I)	EF177175	ALEDADLGGDK, ALEDADLGGDKLSK, LLAGESGIGLIDR, LLAGESGIGLIDRFDASK, RLDDCLR
Beta-ketoacyl-ACP synthetase I (KAS I)	DY910493	ALEHADLAADNR, KALEHADLAADNR
3-keto-acyl-ACP synthase II	DQ835562	ALADAGISPSDSDEIDKSR, VFNDAIEALR
Stearoyl-ACP desaturase	U70374	AKESVNVPFSWIFDR, ATFISHGNTAR, ESVNVPFSWIFDR, HGDLLHQYLYLSGR, VADLTGLSGEGR
Stearoyl-ACP desaturase	U91339	AKEGPSIPFSWIFDR, AQDYVCGLPSR, KAQDYVCGLPSR, LAQICGTIAADEK
Long chain acyl-CoA synthetase 4-like	DY912306	HGPYVWLTYK, QVYDKVIQVGNAIR
Long chain acyl-CoA synthetase	DY911733	AAIGSGLVAHGIPK, VRPDGTVGDYK
Delta-12 oleate desaturase	U91341	ALRPVLGEYYR, FACHYVPTSPMYNER,

		FDKTPFYVAMWR, GALATVDRDYGVLNK, HHSNTGSLERDEVFVPK, YFNNTVGR
Acyl-ACP thioesterase FATA1	AY078350	CYEVGINK, KLNLIWVTSR, SSGEGLELNR, TGVAVDVTEKR, VNDDIRDEYLIFCPK, WVMMNSETR
Acyl-CoA synthetase	GE500285	KVFITDSVPK, RIVAEHFLTR
Phospholipid/glycerol acyltransferase (CDS gene = "ER-GPAT1")	ABU88984	GAFELGATVCPIAIK, IFVDAFWNSR, LRDLLDISPTLTEAAGAIVDDSFTR, PNIEDYLPPDSIQQPHTK
Phosphatidylcholine: Diacylglycerol Acyltransferase	GE497124	AMDPGLLDSEILGLK, SIMNIGPAFLGIPK, TWDSIISLLPK
Degradation		
3-hydroxyacyl-CoA dehydrogenase	DY909264	LGLIDAIAPPQDLLK, TDKIGSLSEAR
3-hydroxyacyl-CoA dehyrogenase	DY909099	FSGGFDINVFQK, LGLIDAIVPPQDLLK, VFNELVLSDTSK
Acetyl Co-A acetyltransferase	GQ254017	TPMGDFLGSLSSLPATK, ILVTLLGVLR, LGSIAIQSALQR
Acetyl-CoA C-acyltransferase/ 3-ketoacyl-CoA thiolase	GE513651	LNVHGGGVSLGHPLGCSGAR, LGLNVIAK
Acyl-CoA dehydrogenase	DY920405	LGALNIAGGTIK, SWYFNHPALDVSK, VEGGWVIEGQKR
Acyl-CoA oxidase	DY907646	MANLVANDPAFEK, VSTHAVVYAR
Delta(3,5)-Delta(2,4)-dienoyl-CoA isomerase, mitochondrial-like	DY916937	LPGIVGFGNAMELALTAR, HMQDAITSIEK

Supplementary Figures

Click here to download E-component(s): Supplementary Figures.docx

Supplementary Tables

Click here to download E-component(s): Supplememnatry Tables.docx

Supplementary Methods

Click here to download E-component(s): Supplementary Methods S1.docx